ACCSCIENCE PUBLISHING

International Journal of Bioprinting

RESEARCH ARTICLE

Roles of pore architecture of artificial bone grafts in invasion competition between bone and fibrous tissue and orientation of regenerated bone

Supplementary File

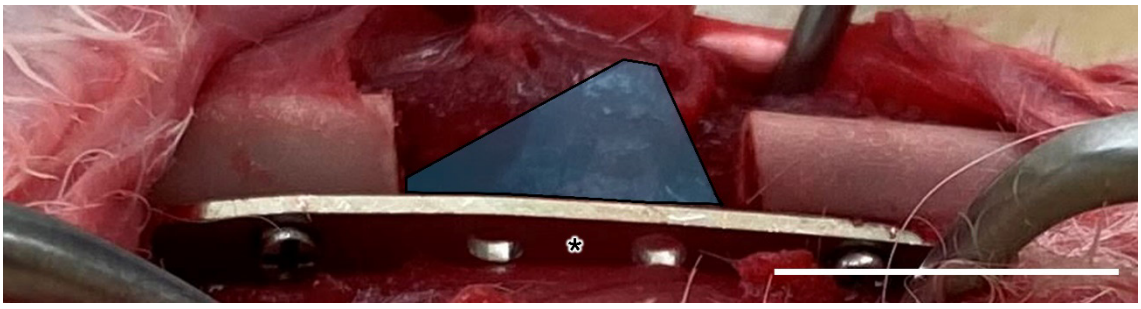

Figure S1. Segmental bone defect model of rabbit ulna (10 mm in length). The osteotomized ulna was fixed with a stainless steel plate and screws (indicated by an asterisk). A polyethylene terephthalate sheet (blue) was placed between the defect and radius. Scale bar: 10 mm.

Table S1. Structural and mechanical characteristics of the L-, S-, and LS-grafts

Parameters	L-graft	S-graft	LS-graft
Uniaxial pore length on a side (μm)	538		
Strut thickness (μm)	325		
Macroporosity (%)	30.7	31.8	36.6
Total porosity (%)	53.6	53.9	59.1
Compressive strength parallel to the pore direction (MPa)	26		8
Compressive strength perpendicular to the pore direction (MPa)	13		

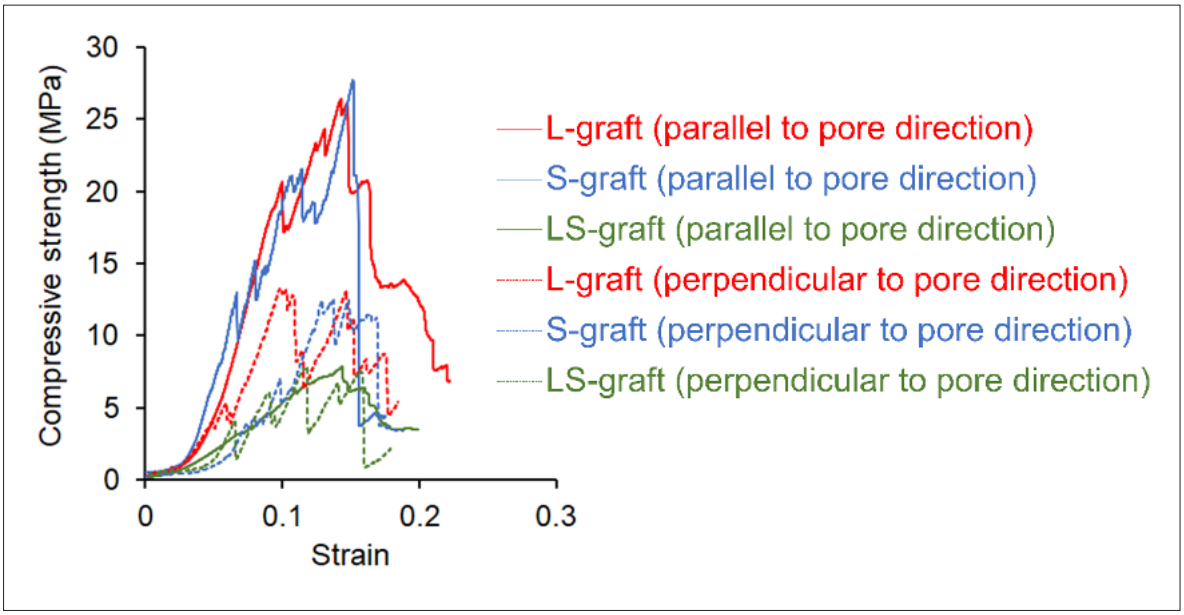

Figure S2. Stress–strain curves of L-, S-, and LS-grafts compressed parallel and perpendicular to the pore direction.

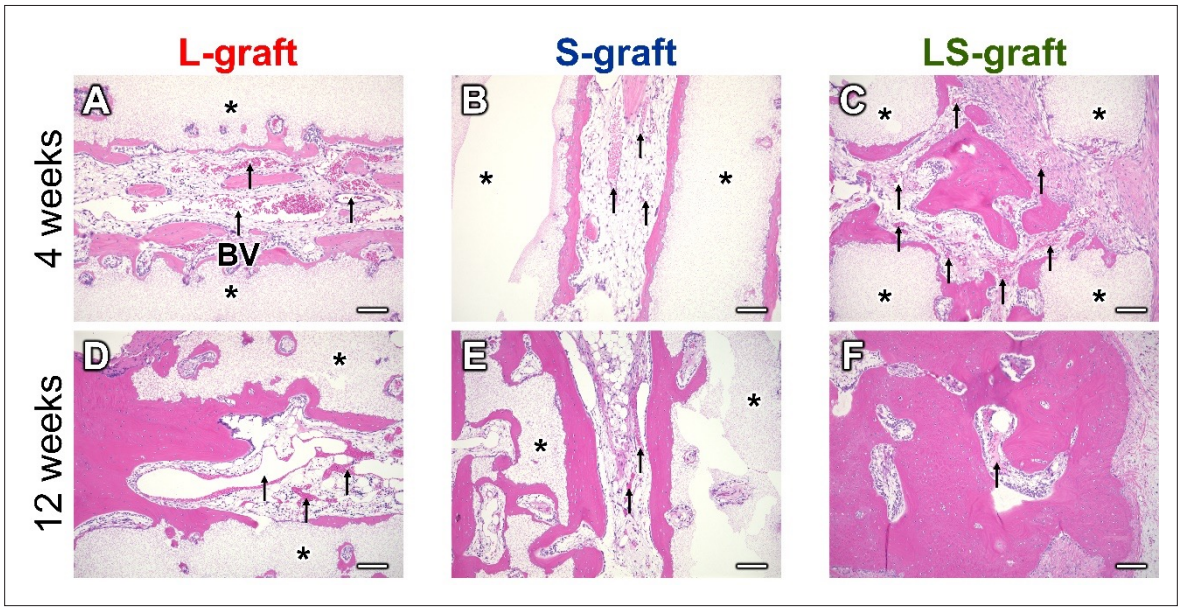

Figure S3. HE-stained images of the new bone area with blood vessels at (A–C) 4 weeks and (D–F) 12 weeks PO. The right and left sides of images show the bone stump sides. The top and bottom of the images show the muscles. The black arrows indicate blood vessels (BV). Scale bars: 100 μm.

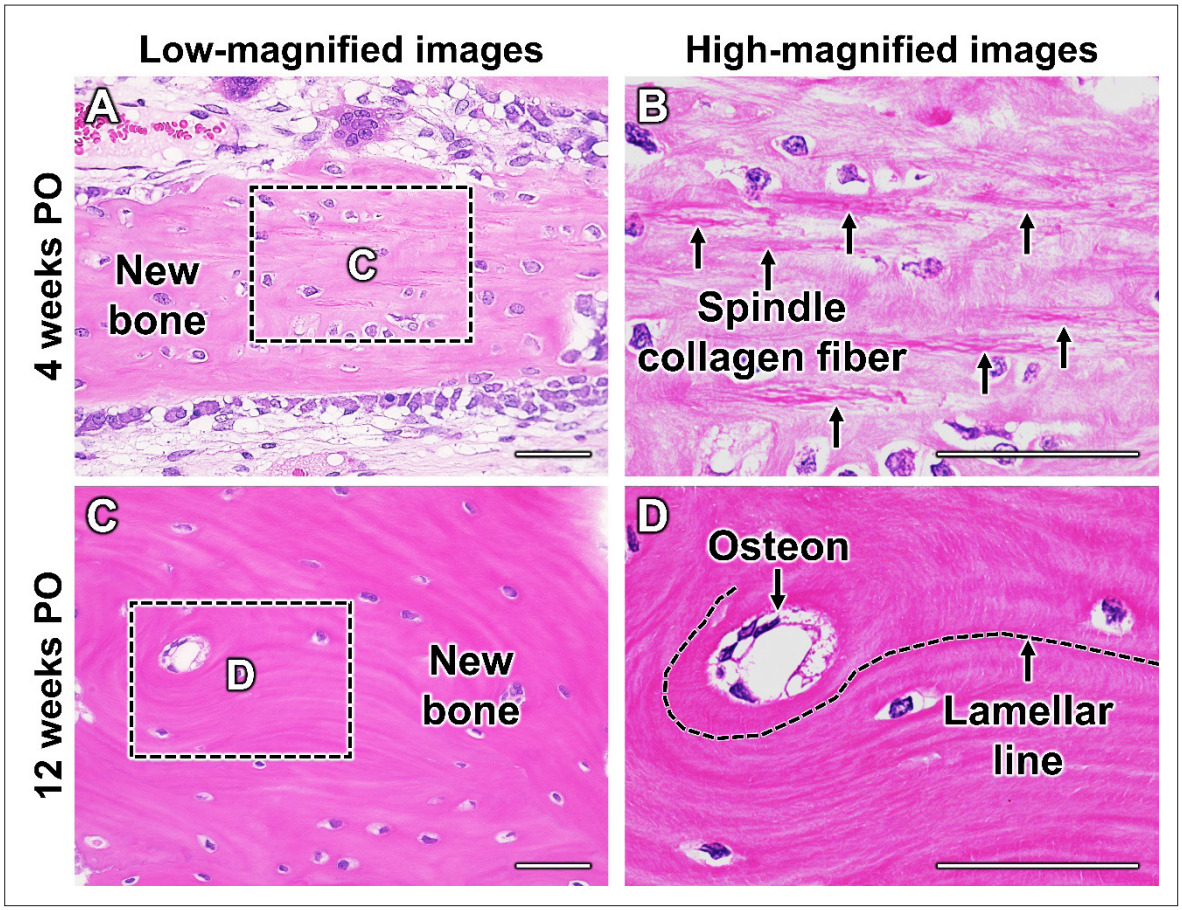

Figure S4. Typical HE-stained images at (A) 4 weeks and (B) 12 weeks PO. (C, D) High-magnified images of (A) and (B), respectively (indicated by black dashed squares). Scale bars: 50 μm.